METAL WASTE FORMS FROM THE ELECTROMETALLURGICAL TREATMENT OF SPENT NUCLEAR FUEL[*]

Daniel P. Abraham
Argonne National Laboratory
Chemical Technology Division
9700 South Cass Avenue
Argonne, Illinois 60439
(708) 252-5486

Sean M. McDeavitt
Argonne National Laboratory
Chemical Technology Division
9700 South Cass Avenue
Argonne, Illinois 60439
(708) 252-4308

Jangyul Park
Argonne National Laboratory
Energy Technology Division
9700 South Cass Avenue
Argonne, Illinois 60439
(708) 252-5030

Submitted for Presentation at
DOE Spent Nuclear Fuel & Fissile Material Management
Embedded Topical Meeting
Spent Nuclear Fuel - Treatment Technologies
Reno, Nevada, June 16-20, 1996

METAL WASTE FORMS FROM THE ELECTROMETALLURGICAL TREATMENT OF SPENT NUCLEAR FUEL

Daniel P. Abraham
Argonne National Laboratory
Chemical Technology Division
9700 South Cass Avenue
Argonne, Illinois 60439
(708) 252-5486

Sean M. McDeavitt
Argonne National Laboratory
Chemical Technology Division
9700 South Cass Avenue
Argonne, Illinois 60439
(708) 252-4308

Jangyul Park
Argonne National Laboratory
Energy Technology Division
9700 South Cass Avenue
Argonne, Illinois 60439
(708) 252-5030

ABSTRACT

Stainless steel-zirconium alloys are being developed for the disposal of radioactive metal isotopes isolated using an electrometallurgical treatment technique to treat spent nuclear fuel. The nominal waste forms are stainless steel-15 wt% zirconium alloy and zirconium-8 wt% stainless steel alloy. These alloys are generated in yttria crucibles by melting the starting materials at 1600°C under an argon atmosphere. This paper discusses the microstructures, corrosion and mechanical test results, and thermophysical properties of the metal waste form alloys.

I. INTRODUCTION

Electrometallurgical treatment refers to the complete set of operations required to break down spent nuclear fuel and convert the radioactive waste constituents into stable forms suitable for disposal. This process involves electrorefining uranium from chopped fuel pins in a molten salt electrolyte[1,2] leaving the TRU and fission product behind. Some metallic components of the spent fuel are inert to the electrorefiner environment and are left behind in the anode baskets after the treatment. These remnant metals constitute the metal waste stream, and include fuel cladding hulls, noble metal fission products, and, in some cases, metallic zirconium from nuclear fuel alloys.[3] These wastes will be stabilized by melting and casting the metals into uniform, corrosion-resistant alloys for eventual disposal in a geologic repository.

Cladding hulls represent the majority (> 90 wt%) of the metal waste stream for every fuel type being evaluated for electrometallurgical treatment. Both stainless steel and Zircaloy clad fuels may be treated, so stainless steel-rich and zirconium-rich waste forms are being developed. The nominal waste form compositions that have been selected are stainless steel-15 wt% zirconium (SS-15Zr) and zirconium-8 wt% stainless steel (Zr-8SS), respectively, with each containing up to 4 wt% noble metal fission products. The addition of external alloying elements to the metal waste form is minimized by using the cladding hulls as the major alloying component.

Stainless steel-zirconium alloys with and without noble metal additions (Ag, Pd, Ru) have been prepared in our laboratory to characterize the properties of the metal waste forms. This paper presents the microstructures of the nominal waste form alloys and discusses the results of corrosion studies, mechanical testing, and thermophysical property measurements.

II. ALLOY PREPARATION

Small-scale samples (~20 g) of stainless steel-zirconium (SS-Zr) alloys were generated using type 304 and 316 stainless steels and high purity zirconium. The presence of noble metal fission products in the waste forms was simulated using additions such as ruthenium, palladium, molybdenum and silver. The starting materials were placed in yttria (Y_2O_3) crucibles, and melted at 1600°C in an argon atmosphere for 1 to 2 hours. Details of the experimental arrangement and melting procedure have been provided elsewhere.[4]

Large-scale (~3 kg) ingots of SS-15Zr alloy were generated in an induction casting furnace attached to a controlled atmosphere glovebox. Type 316 stainless steel and zirconium metal rods were charged into 4 in. (10 cm) diameter yttria crucibles and alloyed at 1600°C under high purity argon for ~1 h. Alloy ingots were made by pouring the melt into casting molds or by slow cooling the melt in the crucible itself. These large-scale alloys have been used to prepare specimens for mechanical and corrosion testing.

III. WASTE FORM CHARACTERIZATION

A. Microstructure and Phase Characterization

Specimens for microscopic examination were sectioned with a diamond saw, cleaned in methanol and polished to a 0.3 μm finish. Initial examination was done with an optical microscope, but most of the analyses were performed using a JEOL 6400 scanning electron microscope (SEM) operating in both secondary and back-scattered electron modes. Standardless quantitative analysis of individual phases was done with an energy dispersive spectrometer (EDS) and Voyager II software from NORAN instruments. The crystal structure of phases was determined by X-ray diffraction; these data were collected with a Philips powder diffractometer using CuK_α radiation.

1. Stainless Steel-rich Alloys. Stainless steel-rich alloy compositions containing from 5 to 35 wt% Zr show varying proportions of the ferritic and austenitic phases of stainless steel and a $ZrFe_2$-type Laves intermetallic, which we have designated $Zr(Fe,Cr,Ni)_{2+x}$.[4] The proportion of $Zr(Fe,Cr,Ni)_{2+x}$ in the alloy microstructure increases with increasing zirconium concentration until, at about 40 wt% Zr, the alloy is almost completely intermetallic. Figure 1 shows a mixture of coarse and fine eutectics typical of a SS-15Zr alloy. The dark regions correspond to a high-chromium ferritic stainless steel phase, whereas the bright regions correspond to the Laves intermetallic phase. Small amounts (<5%) of an austenite phase (face-centered cubic) and a Zr_6Fe_{23}-type intermetallic were also found in the SS-15Zr alloy.
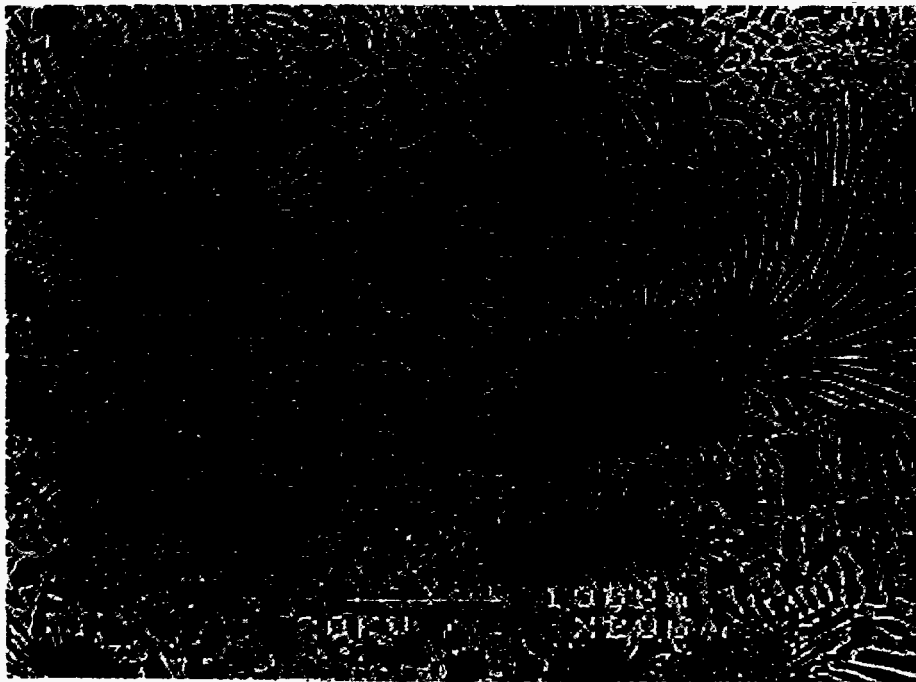

Figure 1. Typical Microstructure of SS-15Zr alloy. The bright phase is the Laves Intermetallic, $Zr(Fe,Cr,Ni)_{2+x}$. The dark phase is ferrite.

The elemental compositions of phases in the SS-15Zr alloy are listed in Table I. The $Zr(Fe,Cr,Ni)_{2+x}$ intermetallic contains only 24 at.% Zr, which is a substoichiometry of more than 25% from the expected 33 at.% Zr. This zirconium substoichiometry is also observed in the Laves phases of ternary Fe-Cr-Zr alloys containing from 5 to 35 wt% Zr. Neutron diffraction studies are being carried out on Fe-Cr-Zr alloys to elucidate the reasons for this zirconium substoichiometry.

Table I. Composition of Phases Observed in SS-15Zr and Zr-8SS Alloys

Alloy	Phases	Relative Proportion	Composition of Major Elements in at.% (± 3%)			
			Fe	Cr	Ni	Zr
SS-15Zr	Ferrite (body-centered cubic)	Major	69	24	4	-
	$Zr(Fe,Cr,Ni)_{2+x}$	Major	54	8	11	24
	Austenite (face-centered cubic)	Very minor	70	20	8	-
	Zr_6Fe_{23}-type	Very minor	57	10	9	19
Zr-8SS	α-Zr solid solution	Major	3	1.5	0.5	94
	$Zr_2(Ni,Fe)$	Minor	28	-	5.7	66
	$Zr(Fe,Cr)_2$	Minor	42	21	-	34

The addition of noble metals does not alter the microstructure of the SS-15Zr alloy. Noble metal additions of Ru, Pd, and Ag were detected in solution for both the intermetallic and ferrite phases. X-ray elemental maps obtained by SEM/EDS revealed that these noble metals exhibit a preference for the Laves intermetallic phase.

The phases observed in the SS-15Zr alloy are in accord with the phases predicted from the Fe-Zr phase diagram.[5] An Fe-15 wt% Zr alloy is close to the eutectic composition and is expected to contain a eutectic of ferrite and $ZrFe_2$. The SS-15Zr alloy also shows a eutectic microstructure; the presence of the eutectic implies that the melting temperature (and hence the processing temperature) is lowest for the 15 wt% Zr alloy.

2. Zirconium-rich Alloys. Zirconium-rich alloy compositions containing from 50 to 92 wt% Zr show a multi-phase mixture of intermetallics and the α-Zr solid solution.[4] The alloys containing 50 and 67 wt% Zr are mainly a mixture of $Zr(Fe,Cr,Ni)_{2+x}$ and a Zr_2Fe-type intermetallic, which we have designated $Zr_2(Ni,Fe)$. The proportion of intermetallic phases in the alloy microstructure decreases, whereas that of the ductile α-Zr increases with increasing zirconium concentration. Figure 2 shows the typical microstructure of a Zr-8SS alloy (92 wt% Zr). The "island-like" features in the figure correspond to the α-Zr phase. The areas between the α-Zr islands contain a mixture of $Zr(Fe,Cr,Ni)_{2+x}$, $Zr_2(Ni,Fe)$, and α-Zr phases.

The elemental compositions of phases in the Zr-8SS alloy are listed in Table I. The α-Zr phase contains ~94 at.% Zr and incorporates minor amounts of Fe, Cr, and Ni. The zirconium content of the $Zr(Fe,Cr,Ni)_{2+x}$ Laves intermetallic is near its stoichiometric value. In addition, the nickel content of this intermetallic is very small; the phase is hence akin to the ternary intermetallic $Zr(Fe,Cr)_2$. The noble metal distribution has not yet been quantified in Zr-8SS alloys.

The zirconium-rich side of the Fe-Zr phase diagram shows a eutectic at about 84 wt% Zr.[5] The melting temperature (and hence the processing temperature) would hence be lowest for an alloy with this zirconium content. The SS-Zr alloys with 84 wt% Zr, however, contain both the Zr_2Fe-type and the $ZrFe_2$-type (Laves) intermetallic phases. Intermetallic-rich alloys are prone to brittleness and may fracture either during fabrication or during storage. Brittle fractures may result in the formation of metallic fines, which increases the alloy surface area and hence the corrosion rate.[6] The Zr-8SS alloy is enriched in the ductile α-Zr phase; this minimizes the probability of brittle fracture and improves the mechanical integrity of the alloy.

B. Corrosion Testing

Corrosion resistance is the primary performance indicator for the metal waste form. A waste form must survive in a repository environment for an extended duration without releasing its inventory of radioactive constituents to the environment. Immersion corrosion tests in simulated J-13 well water (representative of the Yucca Mountain repository) have indicated that both the stainless steel-rich and zirconium-rich waste form alloys are very resistant to general corrosion. These alloys have retained their shiny surfaces even after 10,000 h exposure at 90°C.
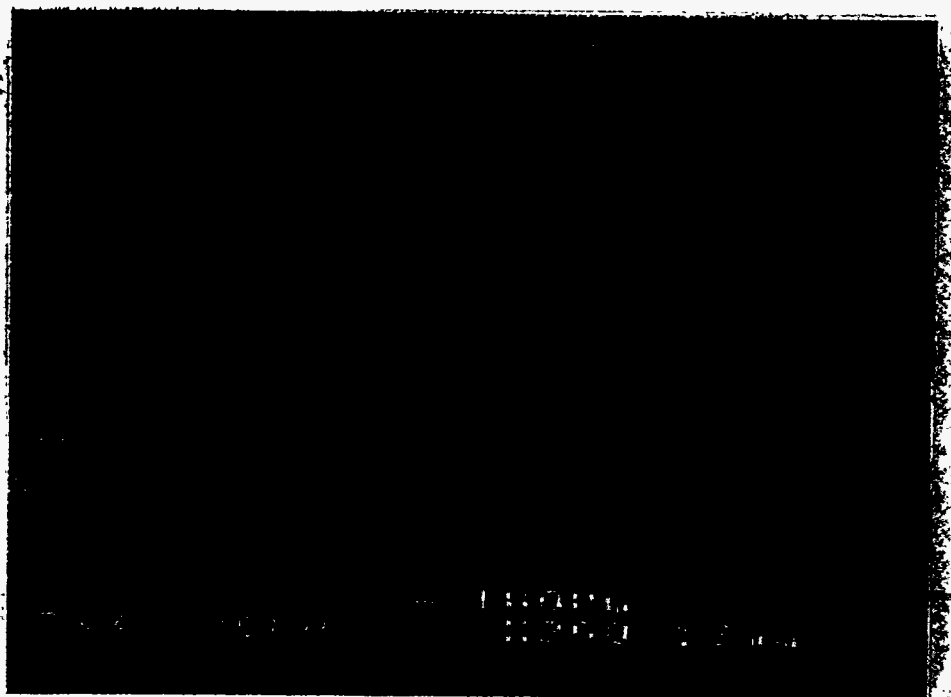
Figure 2. Typical Microstructure of Zr-8SS alloy. The "island-like" features
are the α-Zr solid solution phase. The areas between the α-Zr islands
contain a mixture of Zr(Fe,Cr,Ni)$_{2+x}$, Zr$_2$(Ni,Fe), and α-Zr phases.

Rapid estimates of metal corrosion rates can be obtained by electrochemical techniques. Disk specimens (15.9-mm dia. and 3-mm thick) were polished to a 600 grit finish and tested in simulated J-13 well water by the linear polarization method. The measured corrosion rates are shown in Table II for the waste form alloys with and without noble metals, commercial zirconium and stainless steels, and selected candidate canister materials. Measurements were made at pH = 2, 4, 7, and 10 to cover a range of potential repository conditions.

The corrosion rates for SS-15Zr and Zr-8SS at pH = 7 are about the same as the rates for 316 stainless steel and zirconium metal. Also, noble metal additions do not significantly affect the corrosion rates of the waste form alloys. The measured rates for the waste form alloys are also similar to the rate for Incoloy 825, which is a candidate material for waste form packaging. Additionally, the corrosion rates are smaller than the rate for pure copper (which is a natural analog for the metal waste forms),[7] and two orders of magnitude lower than the rate for mild steel. Corrosion rates for Zr-rich alloys are not affected significantly by pH variations, but increasing acidity increases the corrosion rates for stainless steel-rich alloys; these increased rates, however, are still relatively low.

Table II. Corrosion Rates Measured by the Linear Polarization Method

Alloy	Corrosion Rate (mils per year)			
	pH = 2	pH = 4	pH = 7	pH = 10
SS-15Zr	0.1-0.4	0.08-0.2	0.02-0.08	0.01-0.02
SS-15Zr-2Ru-1.5Pd-0.5Ag	0.4-0.5	0.2	0.04-0.1	0.06-0.09
316 Stainless Steel	0.3	0.05	0.04	0.04
Zr-8SS	0.02-0.08	0.05-0.06	0.02-0.03	0.01
Zr-8SS-1Ru-1Mo-0.5Pd	0.08	0.04	0.03	0.01
Zirconium	0.02	0.05	0.06-0.09	0.07
Incoloy 825	0.03	0.05	0.07	0.03
CDA122 (High-purity copper)	8.9	8.5	0.1-0.2	0.4
A106 Grade B steel	50	23	12	12

C. Thermophysical Properties

Information on thermophysical properties is essential for modeling waste form performance. For example, thermal gradients (and hence thermal stresses) in a waste form may cause fractures during fabrication and long-term storage.[6] The presence of thermal gradients is dictated by the material's thermal conductivity and coefficient of thermal expansion. For the same temperature gradient, thermal stresses are lower in a material with a lower thermal expansion coefficient. Thermal gradients and stresses are also lower in a material with high thermal conductivity.

Preliminary experiments to estimate the thermophysical properties (specific heat, thermal conductivity, and thermal expansion) of the SS-15Zr waste form alloy have been performed at the Thermophysical Properties Research Lab (TPRL), Purdue University. Table III compares the room temperature thermal properties of SS316-15Zr with those of 316 stainless steel, zirconium, and borosilicate glass and Synroc waste forms. The thermal expansion coefficient of SS-15Zr is similar to that for borosilicate glass and Synroc but smaller than that for 316 stainless steel. The thermal conductivity of SS-15Zr is only slightly smaller than the thermal conductivity of 316 stainless steel;

however, it is an order of magnitude larger than the value for borosilicate glass, which has relatively poor thermal conductivity. It is evident from Table III that less heat is required to raise the temperature of the SS-15Zr alloy, but the heat is also conducted away rapidly. Thus, thermal gradients and thermal stress fractures are not expected to occur in the SS-15Zr waste form.

D. Mechanical Properties

Mechanical test specimens for uniaxial tensile testing and impact testing were produced from our large-scale SS-15Zr ingots. The uniaxial tensile test was performed on round bar specimens with a gage length of 1.45 in (3.68 cm); the specimens were loaded at an extension rate of 3×10^{-7} in./sec (8×10^{-7} cm/sec) at 90°C in air. The specimens failed at a tensile fracture stress of ~ 43 ksi (~300 MPa) and showed less than 1% elongation. This fracture stress is approximately 30% higher than that of annealed oxygen-free copper but about 40% lower than annealed Type 316 stainless steel. The SEM examination of the tensile fracture surface showed that brittle cleavage was the dominant fracture process; ductile fracture processes, such as microvoid coalescence, were not observed.

Table III. Thermal Properties of Various Materials

Material	Property (near room temperature values)		
	Thermal Conductivity ($W\,m^{-1}\,K^{-1}$)	Coefficient of Thermal Expansion (K^{-1})	Specific Heat ($J\,g^{-1}\,K^{-1}$)
SS-15Zr	12.2	11.0×10^{-6}	0.45
316 Stainless Steel	14.6	16.5×10^{-6}	0.50
Zirconium	20.0	5.6×10^{-6}	0.28
Borosilicate Glass	1.0	8.1×10^{-6}	0.80
Synroc	2.1	10.5×10^{-6}	0.55

Charpy impact tests were also performed on standard notched-bar SS-15Zr specimens at room temperature. The energy absorbed in fracturing the specimens was ~ 0.8 J/cm^2. Typical cleavage and river patterns were seen on the impact fracture surfaces. The fracture path was mainly through the intermetallic phase, but secondary cracking in the ferrite was also seen. The impact energy of the SS-15Zr alloy is higher than that of simulated nuclear waste glass specimens (0.1 J/cm^2) but much lower than the values for wrought or cast stainless steels, whose impact energies are in the range of 100-200 J/cm^2.

IV. SUMMARY

Metal waste forms from the electrometallurgical treatment will be either a stainless steel-rich or a zirconium-rich alloy, depending on the composition of the cladding hulls being treated. The major phases in the stainless steel-rich alloy, SS-15Zr, are an iron solid solution (ferrite) and an intermetallic, $Zr(Fe,Cr,Ni)_{2+x}$. The major phase in the zirconium-rich alloy, Zr-8SS, is an α-Zr solid solution phase. Small amounts of the Zr_2Fe-type and the $ZrFe_2$-type intermetallic are also present in the Zr-8SS alloy. Noble metal (Ag, Pd, Ru)

additions do not alter the microstructure of the SS-15Zr alloy; all the noble metal elements are dissolved and distributed in the intermetallic and ferrite phases. Both alloy waste forms show excellent resistance to corrosion and exhibit favorable mechanical properties.

V. ACKNOWLEDGMENTS

VI. REFERENCES

1. J. E. Battles, J. J. Laidler, C. C. McPheeters, and W. E. Miller, "Pyrometallurgical Processes for Recovery of Actinide Elements," *Actinide Processing: Methods and Materials*, B. Mishra and W. A. Avrill, eds., pp. 135-151, TMS Publications, Warrendale, Pennsylvania (1994).

2. E. C. Gay and W. E. Miller, "Electrorefining N-Reactor Fuel," *Proc. DOE Spent Nuclear Fuel-Challenges and Initiatives*, Salt Lake City, Utah, December 13-16, 1994, pp. 267-274, American Nuclear Society, La Grange Park, Illinois (1994).

3. S. M. McDeavitt, J. Y. Park, and J. P. Ackerman, "Defining a Metal-based Waste Form for IFR Pyroprocessing Wastes," *Actinide Processing: Methods and Materials*, B. Mishra and W. A. Avrill, eds., pp. 305-319, TMS Publications, Warrendale, Pennsylvania (1994).

4. D. P. Abraham, S. M. McDeavitt, and J. Y. Park, "Microstructure and Phase Identification in Type 304 Stainless Steel-Zirconium Alloys," submitted to *Metall. and Mater. Trans.* (1995).

5. D. Arias and J. P. Abriata, "Fe-Zr," *Binary Alloy Phase Diagrams*, vol. 2, T. P. Massalski, ed., pp. 1798-1800, ASM International, Materials Park, Ohio (1990).

6. W. Lutze and R. C. Ewing, "Summary and Evaluation of Waste Forms," *Radioactive Waste Forms for the Future*, W. Lutze and R. C. Ewing, eds., pp. 699-740, North Holland, Amsterdam (1988).

7. B. Miller and N. Chapman, "Postcards from the Past: Archaeological and Industrial Analogs for Deep Repository Materials," *RadWaste Magazine*, pp. 32-42 (January 1995).

DISCLAIMER